Alloying of Fe-Al-Si Alloys by Nickel and Titanium

Kateřina Nová, Pavel Novák, Adrian Arzel, Filip Průša
University of Chemistry and Technology, Prague, Department of Metals and Corrosion Engineering, Technická 5, Praha 6, Czech Republic, novakx@vscht.cz

This paper focuses on one part of the otherwise very complex research of intermetallic compounds based on Fe-Al-Si at the UCT Prague. These materials seem to be suitable candidates for use in extreme conditions (high temperatures, oxidation and sulfidation environment, ...), especially in the aerospace and automotive industries. The aim of this work was to describe the influence of alloying elements - Ni and Ti on phase composition, microstructure, mechanical and oxidative properties, in two specific systems - FeAl35Si5 and FeAl20Si20 (in weight %).

Keywords: Intermetallics, Mechanical properties, Powder metallurgy, Spark Plasma Sintering

1 Introduction

Intermetallics are compounds with a large variety of chemical compositions. These alloys are made up of two or more metals where the resulting crystallographic structure is different from each of the input metals. The very large variability of chemical composition and production possibilities allows to prepare materials suitable for use in the automotive or aerospace industry as well as power generation or medicine [1, 2].

Particularly for aerospace industry or powder plants there are usually used conventional iron- or nickel-based heat resistance alloys. However, global economic situation and the low availability of some elements brings a challenge in the production of a variety of materials without content critical raw materials (CRM) like tungsten, cobalt and chromium [3]. Silicon, even though it is listed as CRM in EU for this year [4], can be used from recycled sources, because the highest purity is not required for these purposes in. In recent years, material based on Fe-Al-Si, which can substitute just CRM for high-temperature applications, was and still is being studied at UCT Prague [5-9].

Potential uses of binary intermetallic Fe-Al alloys are significant in the chemical and automotive industries, including heat exchangers, catalytic converters, exhaust valves and gas filters [10-12]. Some articles also deal with the influence of other alloying elements [13, 14]. For example, the addition of silicon to the Fe-Al matrix leads to increase the brittleness of the material. But on the other hand, oxidation resistance and thermal stability is improved with the addition of silicon [6, 15]. Alloys based on Fe-Al-Si are desired for use in severe conditions, which require high wear-resistance and as mentioned above thermal stability at elevated temperature.

Ternary phase diagrams are often very complex and an understanding of them and the thermodynamic properties is fundamental to the control of the microstructure and phases composition formed during solidification. Just these characteristic have significant effect on the final properties of the material. In the field of production there wasn´t much room for improvement, because methods of powder metallurgy including Spark plasma sintering allows to prepare high purity of products with precise chemical composition, as well as nanocrystalline microstructure with a density close to the theoretical density, it means with a very low proportion of porosity [16-18]. Therefore, the research focused on the change in chemical composition. It was assumed that the next required improvement of mechanical properties would occur if the matrix will not form a ternary phase, as it is the case of FeAl20Si20 intermetallic alloy. Depending on the knowledge of the Gibbs' energies of formation (Tab. 1) [19], the nickel was added as an aluminide-forming element which, at the assumed compaction temperature (1000 ° C = 1273.15 K), is supposed to bind aluminium from the material, and then the matric would be formed by iron silicides. On the same principle, the titanium was chosen as the second alloying elements, because it is strongly silicide-forming, thus forming a phase with silicon, and the matrix will be purely based on iron aluminides.

Tab. 1 *Gibbs' energies of formation of selected intermetallic phases [19]*

	ΔG_f (1300K) [kJ/mol]		
TiSi	TiAl	NiSi	NiAl
-129.06	-62.16	-81.50	**-101.39**

2 Experimental

In the first steps of produce compact sample was prepared powder mixtures, contained FeXAl20Si20Ni/TiX-Y and FeXAl35Si5Ni/TiX-Y (in weight %), where Y = 0 or 20. It was based on commercially available pure powders, which were mechanically alloyed by planetary ball mill Retch PM 100 CM in a stainless steel container (ball-to-powder ratio of 15:1) for 10 h at 400 rpm, change of rotation direction each 30 min. The process was under a protective argon atmosphere (purity of 99.996 %) to prevent oxidation. The obtained powders were compacted to 20 mm diameter cylindrical samples by the means of SPS under the following conditions: sintering temperature of 1000 °C, heating rate of 300 °C.min^{-1} to 900 °C and then 100 °C.min-1 to 1000 °C, 10 min at the sintering temperature, pressure of 48 MPa. The sample was then slowly cooled in the chamber (50 °C.min^{-1}) to prevent its cracking.

Metallographic samples were prepared by grinding at sandpapers with SiC particles (P80 - P2500) and then the

samples were polished using D2 and D0.7 diamond paste. Microstructure of all samples was investigated after etching by modified Kroll's reagent (10 ml HNO_3, 5 ml HF, 85 ml H2O) on TESCAN VEGA 3 LMU scanning electron microscope equipped with Oxford Instruments X-max 20 mm2 EDS detector with Aztec software package.

The phase composition of samples was examined by X-ray diffraction (XRD) analysis using PANalytical X'Pert Pro diffractometer (CuKα radiation with the wavelength of 0.154060 nm) using the HighScore Plus software and the relevant PDF2 database.

Mechanical properties were measured on compact samples by means of the universal testing machine Lab-Test 5.250 SP1-VM. The device is equipped with a laser extensometer for the accurate measurement of deformation of the sample. Tests were performed at compact samples at room temperature and at elevated temperature, namely 800 °C. Vickers microhardness with a load of 1 kg (HV 1) was measured on a standard hardness meter.

3 Results and discussion

From the Tab. 2, we can see that the binary phases were detected only for alloys FeAl35Si5Ni/Ti20. In the case of FeAl35Si5Ni20 alloy, the composition is very simple and the material is made up of aluminides. In the second alloy with a lower content of silicon alloyed by titanium, several types of silicides and also titanium and iron aluminides were found. For alloys with higher silicon content (see Tab. 2, or Fig. 1), there was always one ternary phase. However, the ternary phase was of a different chemical composition and crystallographic structure than in the ternary Fe-Al-Si alloys.

SEM micrographs (Fig. 2) show the difference in the effect of the alloying elements. While nickel alloys have a very fine and almost homogeneous structure, with the addition of titanium there is a grain coarsening observed.

Tab. 2 *Phase composition of compact samples*

	Phase composition				
FeAl35Si5	FeAl	Fe_3Si			
FeAl35Si5Ni20	NiAl	Fe_3Al			
FeAl35Si5Ti20	FeAl	Ti_5Si_4	Ti_5Si_3	$TiSi_2$	Ti_3Al
FeAl20Si20	Fe_3Si	FeSi	$Fe_3Al_2Si_3$		
FeAl20Si20Ni20	Fe_3Si	Al_3Ni_2	$AlNi_2Si$		
FeAl20Si20Ti20	FeAl	FeSi	Ti_5Si_3	FeTiSi	

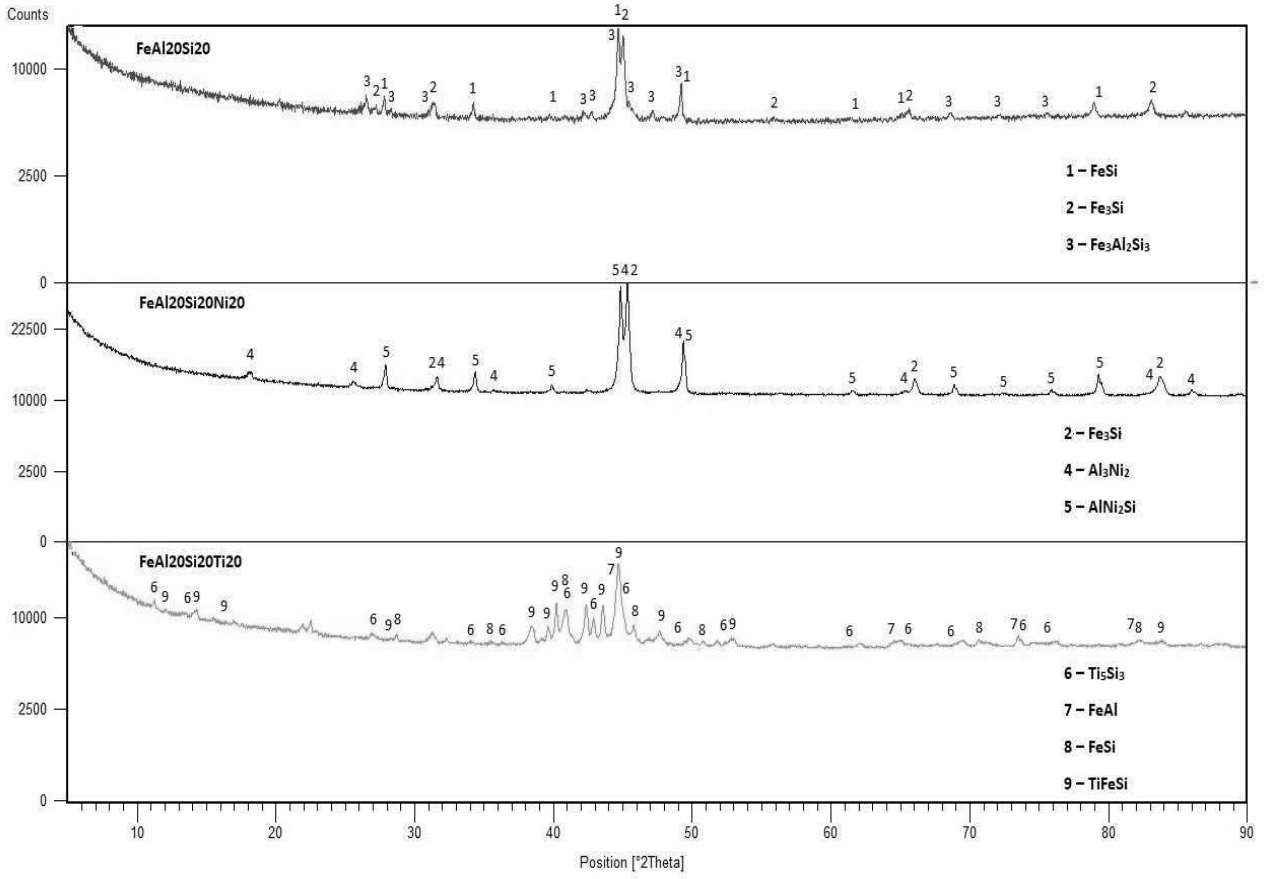

Fig. 1 *Phase composition vs. chemical composition for alloys FeXAl35Si5Ni/TiX-Y*

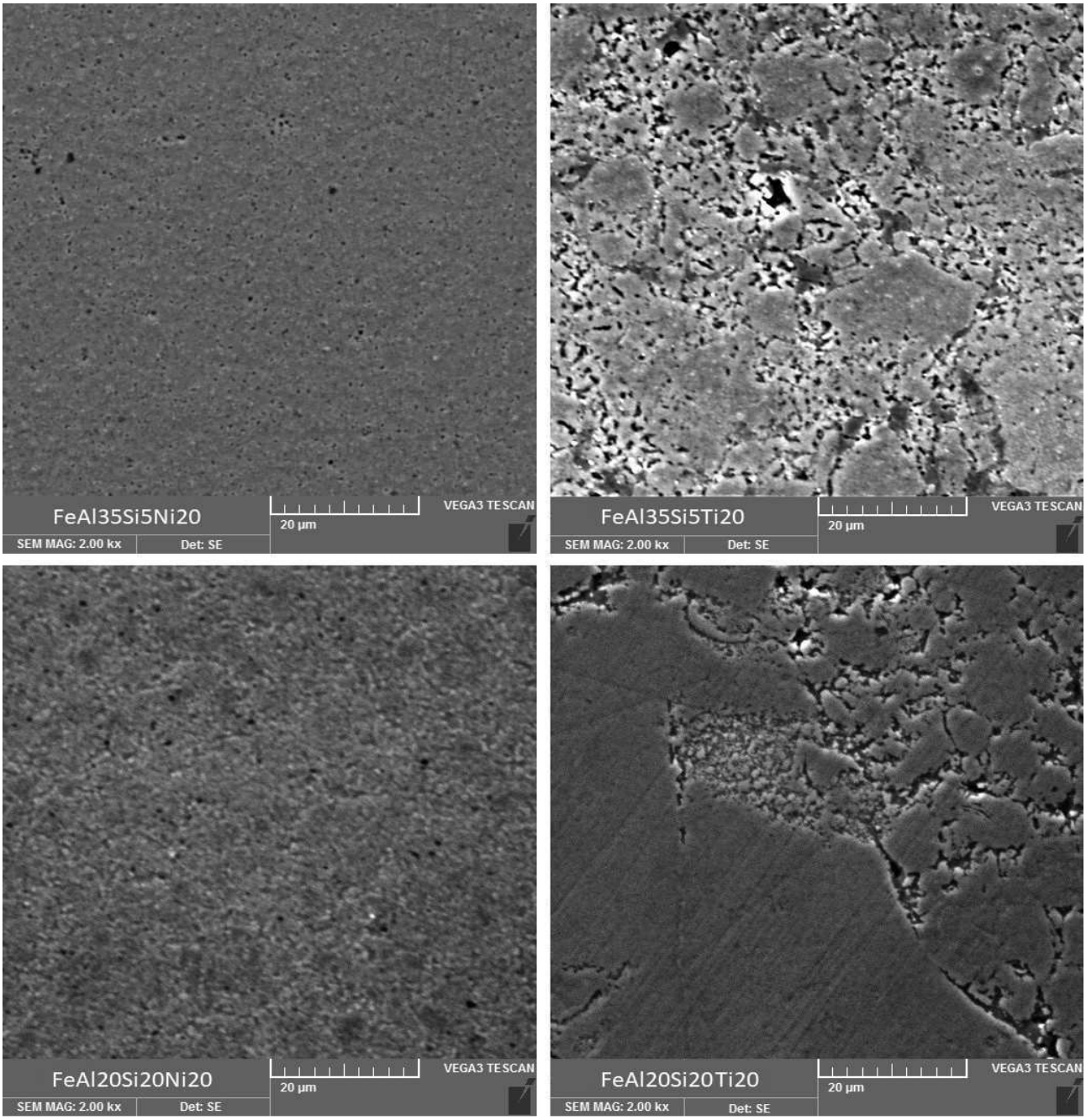

Fig. 2 *Microstructure of tested FeAlSiNi/Ti alloys*

Fig. 3 shows the stress–strain curves at room temperature. The plastic area was not observed in any of the tested materials and also the measurement was determined by the fracture of samples. So it means that all of the materials are brittle at room temperature. A similar shape of the curve was observed for FeAl20Si20 alloy without additional alloying elements, which also exhibited an almost negligible degree of plastic deformation and ultimate compressive strength of 1085 MPa. About with nickel or titanium, the highest values were measured for alloy FeAl20Si20Ni20, which ultimate compressive strength was more than 1800 MPa. On the other hand, it is interesting, that the second sample prepared by same process and also with the same composition achieved worse values at the end.

Curves for both samples of FeAl35Si5Ni20 were almost identical, but from the figure it is evident that the first material failure occurred already at 1450 MPa, however the total material failure was occurred at value of stress about 100 MPa higher. It could be caused by residual porosity or by difference in mechanical properties of present phases. Black curves represent the alloy FeAl20Si20Ti20, the measurement had the expected course and the resulting values for both samples were comparable. A big difference in measured values can be seen with the last alloy – FeAl35Si5Ti20. Already with the previous measurements, we have made sure that the results are greatly influenced by the quality of the sample preparation. Surface irregularities, some manufacturing defects, imperfections in the sample geometry have a major impact on results.

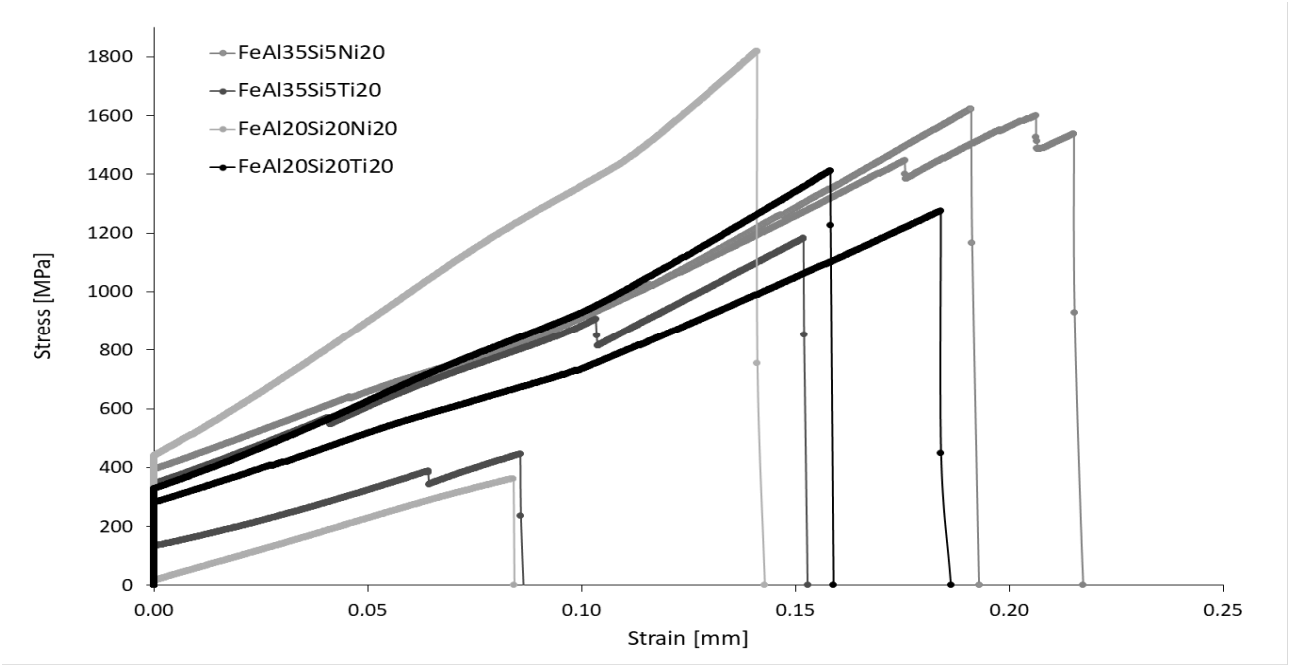

Fig. 3 *Stress-strain curves at room temperature (25 °C)*

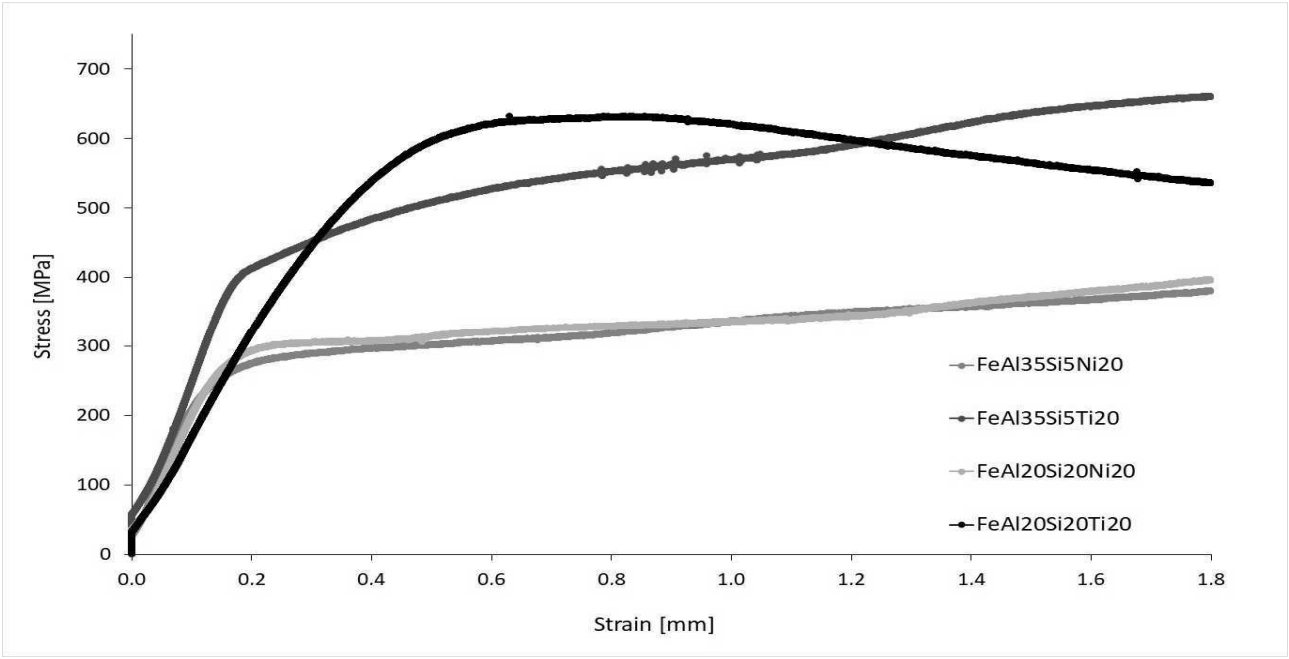

Fig. 4 *Stress–strain curves at room temperature (800 °C)*

In the contrast with Fig. 3, in the following figure (see Fig. 4), it is evident that the blocks prepared from all alloys were constantly compressed and deformed, but they didn´t break through the fracture during measurement at an elevated temperature, namely 800 °C. The increasing stress during each test, except alloy FeAl20Si20Ti20, means strain hardening also known as work hardening of the materials. This strengthening occurs because of the mutual interaction of dislocations, which causes the formation of barriers and thus prevents dislocation movements. The grain boundary sliding is not possible under the test conditions, thus the material becomes stronger and more difficult to deform. For alloy FeAl20Si20Ti20 strain hardening wasn´t observed. At the same time it is visible from the picture that alloy with nickel have almost identical curves.

Tab. 3 shows results of microhardness. A relatively large scattering of the measurement is evident, which can be explained by the selected load. Hardness depends on the location of indentation due to heterogeneity of the structure. The hardness of the aluminide phase is lower than that of silicides. The indentation could also cross the boundary. Furthemore, both nickel-containing alloys had a much finer microstructure, so their higher hardness was assumed, but as mentioned above, the alloy FeAl35Si5Ni20 was formed only by aluminides, therefore having lower hardness. The reason for high hardness for alloy with titanium probably lies in the large number of phase boundaries and a large amount of hard silicides in the matrix.

Tab. 3 Microhardness

Alloys	HV1
FeAl35Si5	907.1 ± 21.6
FeAl35Si5Ni20	972.3 ± 42.0
FeAl35Si5Ti20	1062.9 ± 91.2
FeAl20Si20	1049.1 ± 57.1
FeAl20Si20Ni20	1375.7 ± 74.1
FeAl20Si20Ti20	1277.5 ± 43.0

4 Conclusion

The original intention to prepare only binary alloys was unfortunately not fully respected. Binary phase composition was confirmed just for alloy based on FeAl35Si5, where addition of titanium or nickel doesn´t lead to the formation of the ternary phase. However, the amount of the ternary phase was minimized in all cases and in addition, the observed ternary phases are not from the range of known brittle Fe-Al-Si phases. The presented results indicate that after addition of alloying elements – Ni and Ti, the hardness increases for all cases. During measurement of compression tests it was confirmed that precise preparation of test specimens is therefore essential. The conclusion can be said that the present ternary phase does not have a detrimental influence on the material properties.

Acknowledgement

This research was financially supported by Czech Science Foundation, project No. 17-07559S and MŠMT No. 20-SVV/2018.

References

[1] PENG, H. (2013). 8 - Brazing of nickel, ferrite and titanium–aluminum intermetallics, In: *Advances in Brazing*, D.P. Sekulić, Editor, Woodhead Publishing. p. 221-248.

[2] NOVÁK, P., LEJČEK, P. (2008). Fyzika kovů. Vysoká škola chemicko-technologická v Praze: Praha.

[3] VODIČKOVÁ, V., ET AL. (2018). High temperature properties of non-critical Fe-Al alloys doped by non critical or "slightly–critical" elements. IOP Conference Series: *Materials Science and Engineering*, Vol: 329(1): p. 012007.

[4] https://ec.europa.eu/growth/sectors/raw-materials/specific-interest/critical_fr. [cited 2018-08-20].

[5] PRŮŠA, F., ET AL. (2015). Structure and mechanical properties of Al–Si–Fe alloys prepared by short-term mechanical alloying and spark plasma sintering. In: *Materials & Design*, Vol. 75, pp. 65-75.

[6] NOVÁK, P., ET AL. (2014). Microstructure Evolution of Fe-Al-Si and Ti-Al-Si Alloys during High-Temperature Oxidation. In: *Materials Science Forum*, Vol: 782: p. 353-358.

[7] NOVÁK, P., ET AL. (2010). Intermediary phases formation in Fe–Al–Si alloys during reactive sintering. In: *Journal of Alloys and Compounds*, Vol: 497(1): p. 90-94.

[8] NOVÁ, K., ET. AL. (2018). The effect of production process on properties of FeAl20Si20. In: *Manufacturing Technology*, Vol: 18(2), p. 295-298.

[9] VALALÍK, M., NOVÁK, P., KUBATÍK, T.F., VOJTĚCH, D. (2015). Unconventional Method of Preparation Intermetallic Phases Fe-Al by Mechanical Alloying in Comparison to Reactive Sintering. In: *Manufacturing Technology*, Vol. 15(1,) p. 105-109.

[10] SCHMITT, A., ET AL. (2017). Creep of binary Fe-Al alloys with ultrafine lamellar microstructures. In: *Intermetallics*, Vol: 90: p. 180-187.

[11] STOLOFF, N.S. (1998). Iron aluminides: present status and future prospects. In: *Materials Science and Engineering: A*, Vol. 258, No. 1–2, pp. 1-14.10.

[12] DEEVI, S.C., SIKKA, V.K., AND LIU, C.T., (1997). Processing, properties, and applications of nickel and iron aluminides. In: *Progress in Materials Science*, Vol: 42(1): p. 177-192.

[13] HADEF, F. (2016). Solid-state reactions during mechanical alloying of ternary Fe–Al–X (X=Ni, Mn, Cu, Ti, Cr, B, Si) systems: A review. In: *Journal of Magnetism and Magnetic Materials*, Vol. 419, pp. 105-118.

[14] COUPERTHWAITE, R.A., CORNISH, L.A. and MWAMBA, I.A. (2016) Cold-spray coating of an Fe-40 at.% Al alloy with additions of ruthenium. *J. S. Afr. Inst. Min. Metall*. [online – cited 2018-08-20]. Vol. 116, p. 927-934.

[15] NOVÁK, P., ET AL. (2011). Oxidation resistance of SHS Fe–Al–Si alloys at 800 °C in air. In: *Intermetallics*, Vol: 19: p. 1306-1312.

[16] RUDINSKY, S., ET AL. (2015). Spark plasma sintering of an Al-based powder blend. In: *Materials Science and Engineering: A*, Vol. 621, pp. 18-27.

[17] PRŮŠA, F., ET AL. (2017). Příprava ultrajemnozrných nanokrystalických materiálů mechanickým legováním a slinováním v plazmatu. In: *Chemické listy*, Vol. 111, pp. 314-321.

[18] TSUKERMAN, S.A. (1965). INTRODUCTION, in *Powder Metallurgy*. Pergamon. p. vii-xi.

[19] BARIN, I. (2008). *Thermochemical data of pure substances*. Wiley-VCH Verlag GmbH, 3rd edition.

10.21062/ujep/154.2018/a/1213-2489/MT/18/4/645